

## ROTATION, CONVECTION, AND MAGNETIC ACTIVITY IN LOWER MAIN-SEQUENCE STARS

R. W. NOYES,<sup>1</sup> L. W. HARTMANN,<sup>1</sup> S. L. BALIUNAS,<sup>1</sup> D. K. DUNCAN,<sup>2</sup> AND A. H. VAUGHAN<sup>3</sup>

Received 1983 June 6; accepted 1983 October 5

## ABSTRACT

Rotation periods are reported for 14 main-sequence stars, bringing the total number of such stars with well-determined rotation periods to 41. It is found that the mean level of their Ca II H and K emission (averaged over 15 years) is correlated with rotation period, as expected. However, there is a further dependence of the emission on spectral type. When expressed as the ratio of chromospheric flux to total bolometric flux, the emission is well correlated with the parameter  $P_{\text{obs}}/\tau_c$ , where  $P_{\text{obs}}$  is the observed rotation period and  $\tau_c(B-V)$  is a theoretically-derived convective overturn time, calculated assuming a mixing length to scale height ratio  $\alpha \sim 2$ . This finding is consonant with general predictions of dynamo theory, if the relation between chromospheric emission and dynamo-generated magnetic fields is essentially independent of rotation rate and spectral type for the stars considered. The dependence of mean chromospheric emission on rotation and spectral type is essentially the same for stars above and below the Vaughan-Preston "gap," thus casting doubt on explanations of the gap in terms of a discontinuity in dynamo characteristics.

*Subject headings:* Ca II emission — convection — stars: late-type — stars: magnetic — stars: rotation

## I. INTRODUCTION

In recent years it has become apparent that there is a strong positive correlation between stellar rotation rate and overall chromospheric activity levels in stars with subsurface convection zones. Such a correlation was first suggested by Kraft (1967), and subsequent work by many authors has led to a widely accepted picture of stellar spindown with age, in which chromospheric Ca II emission decreases along with the stellar surface rotation rate. The large body of work leading up to this view has recently been reviewed by Skumanich and Eddy (1981). Recent analyses of X-ray data (e.g., Pallavicini *et al.* 1981; Walter 1981, 1982) show that coronal emission also is linked to rotation. In the Sun, both chromospheric and coronal emission are known to be well correlated with surface magnetic fields, and as a result the correlation may be interpreted as reflecting a close relation between overall level of surface magnetic activity (that is, total magnetic flux at the surface) and stellar rotation rate. Such a relation is to be expected on the basis of standard dynamo theory, which predicts increasing field amplification with increasing rotation and differential rotation (see, for example, monographs by Moffat 1978, Parker 1979, and Krause and Radler 1980).

Rotation is not the only parameter expected to influence stellar surface magnetic activity; another is the stellar mass, or equivalently, main-sequence spectral type, which dictates the properties of the stellar convection zone. In particular, the depth of the convection zone, or its convective overturn time, is thought to play a role in the dynamo regeneration of magnetic fields. It is expected that stars of later spectral types (that is, with deeper convection zones relative to their radius) will show stronger dynamo behavior than stars of earlier

spectral type, for a given rotation period. This expectation is borne out, qualitatively at least, by X-ray data: Vaiana *et al.* (1981) find that the ratio of X-ray to bolometric luminosity in K and M dwarfs increases steadily with advancing spectral type, even though surface rotation decreases with advancing spectral type along the lower main sequence (Vaughan *et al.* 1981). Walter (1981) found that G8-K5 main-sequence stars show a factor of 10 greater value of X-ray luminosity relative to bolometric luminosity than do F8-G5 stars with the same rotation rate.

Chromospheric emission may be expected to show a qualitatively similar dependence on convective zone depth or turnover time. However, Catalano and Marilli (1983) found a correlation between Ca II emission flux and rotation of lower main-sequence stars, without any apparent dependence on spectral type. A similar result was found by Middelkoop (1982). On the other hand, Noyes (1983) found that Ca II emission levels (normalized to bolometric emission) could be approximated as the product of the angular rotation rate and an additional functional of spectral type alone. He noted that the function of spectral type had approximately the same shape as the convective overturn time calculated from standard interior models. This suggested that the inverse of the Rossby number, that is the product of angular rotation rate and convective overturn time, may be the governing parameter determining stellar surface magnetic activity.

In the present paper we carry this idea further by explicitly determining the dependence of Ca II emission on rotation and spectral type. We consider only lower main-sequence stars (that is, main-sequence stars of spectral type F or later), for which accurate values of mean Ca II emission flux and rotation periods exist. We have found that the chromospheric emission, expressed as a fraction of the bolometric luminosity, is rather well described by the single parameter  $Ro$ , where  $Ro = P_{\text{obs}}/\tau_c$  and  $\tau_c$  is a function of spectral type alone. The functional form  $\tau_c(B-V)$  is essentially identical to the convective overturn time near the bottom of the convection zone, as calculated

<sup>1</sup> Harvard-Smithsonian Center for Astrophysics.

<sup>2</sup> Mount Wilson and Las Campanas Observatories, Carnegie Institution of Washington.

<sup>3</sup> Perkin-Elmer Corporation, and Mount Wilson and Las Campanas Observatories.

by Gilman (1980) from convection zone models, assuming a ratio  $\alpha = 2$  of mixing length to scale height. We take this as suggestive that the Rossby number  $P/\tau$  is in fact a major determinant of surface magnetic activity in lower main-sequence stars.

In § II, we present and discuss the data underlying this study. Section III contains our analysis, and we discuss the implications of this analysis in § IV.

## II. THE DATA

### a) Chromospheric Emission Level

The basic data are observed flux indices  $S$  for the Ca II H and K lines, as measured with the Mount Wilson H-K spectrophotometer (Vaughan, Preston, and Wilson 1978). Our underlying assumption is that the summed Ca II H and K (hereafter denoted HK) flux reflects the amount of nonthermal chromospheric heating, which in turn is associated with surface fields. This assumption is validated, for the Sun at least, by a large body of previous observations (e.g., Leighton 1959; Skumanich, Smythe, and Frazier 1975).

Little or no data exist to aid in a quantitative extension of the above assumption to stars of different spectral types. In comparing stars of different spectral types, we shall use the parameter  $R'_{\text{HK}}$ , defined as the ratio of the emission from the chromosphere in the cores of the Ca II H and K lines to the total bolometric emission of the star. (The prime denotes subtraction of a photospheric contribution to the observed H and K emission, as we describe below.) This choice of parameter is made plausible by noting that  $R'_{\text{HK}}$  is proportional to that fraction of the nonradiative energy flux in the convective zone (essentially equal to the entire stellar bolometric luminosity throughout most of the convection zone) which is ultimately converted into magnetic field-associated chromospheric heating.

The observed Ca II H and K flux index, from which we shall derive the chromosphere emission ratio  $R'_{\text{HK}}$ , shows large time variations. These are due to fluctuations of emission on all time scales including times short compared to rotation (Baliunas *et al.* 1981), rotational modulation at the stellar rotation period (Vaughan *et al.* 1981), and long-term variations in overall activity level (Wilson 1978). We are concerned in this paper with the *mean* level of activity induced in the convection zone of a rotating star, and not in fluctuations which occur over time scales short compared to the time scale over which rotation or convective properties change. In order to minimize uncertainties introduced by such fluctuations, we have restricted our attention to stars in the long-term activity survey of Wilson (1978). These stars have been observed approximately monthly during each observing season since 1966, and in most of the cases discussed here, much more intensively since 1980. From the totality of data for each star, we have determined a mean value  $\langle S \rangle$  by selecting a level halfway between the minimum and maximum of a line hand-drawn through the seasonally varying values, from 1966 to the present, in Wilson's (1978) data and its extension. In this procedure we deleted extreme data points due to short-term activity fluctuations or measurement errors. Table 1 lists the stars in the present study, with the values of  $\langle S \rangle$  used given in the fourth column.

The quantity  $\langle S \rangle$  is plotted versus  $B-V$  in Figure 1. The

"gap" first pointed out by Vaughan and Preston (1980) is quite evident, as a diagonally slanted region nearly devoid of points separating stars with higher mean HK emission levels from those of lower HK emission. Open and closed symbols represent stars labeled "old" and "young" respectively by Vaughan (1980), by virtue of their location above and below the gap. The membership of individual stars in these two classes is given in the ninth column of Table 1.<sup>4</sup>

The quantity  $\langle S \rangle$  is defined (Vaughan, Preston, and Wilson 1978) as proportional to the ratio of measured flux within the 1 Å H and K bandpasses of the Mount Wilson H-K photometer to that in two continuum windows equidistant to the red and violet of the H and K lines. It is sensitive to the integrated emission over these windows, which is very dependent on spectral type. It is also sensitive to the amount of photospheric radiation transmitted by the H and K instrumental passbands. To determine the level of true chromospheric emission in the H and K lines quantitatively, it is necessary to correct for both of these effects.

Middelkoop (1982) has derived a color-dependent conversion factor  $C_{\text{cf}}(B-V)$  which converts the flux index  $S$  into the quantity  $R_{\text{HK}} = C_{\text{cf}} \times S$  and thereby has corrected for the variation with  $(B-V)$  of the amount of photospheric radiation in the continuum windows. Here  $R_{\text{HK}} = F_{\text{HK}}/(\sigma T_{\text{eff}}^4)$ , where  $F_{\text{HK}}$  is the total flux per cm<sup>2</sup> at the stellar surface in the H and K passbands. This conversion factor was obtained by comparing measured fluxes in the red and violet continuum channels for a number of stars in the solar neighborhood with their known visual magnitude, and applying suitable bolometric corrections. Because the data used by Middelkoop were not obtained by absolute spectrophotometry, we have checked this calibration using other spectrophotometry. This procedure is described in the Appendix. We find that Middelkoop's conversion factor is quite consistent with independent spectrophotometric measurements for  $B-V \leq 1.0$ , and so we use it here, with only a very small modification for stars with  $B-V \lesssim 0.6$ . The details of the conversion relation actually used are also given in the Appendix. It should be noted that the calibration for  $B-V > 1.0$  may be uncertain by as much as 20% (see the Appendix). Values of  $\langle R_{\text{HK}} \rangle$  are given in the fifth column of Table 1.

Next we must correct for the fraction of the total emission within the H and K passbands which is photospheric, rather than chromospheric in origin. From solar observations (e.g., White and Livingston 1981) we know that emission in the wings of the H and K lines (that is, outside the H1 and K1 minima in the line profiles), which is primarily photospheric in origin, is much less enhanced over magnetic active regions than is the chromospheric emission in the line cores. Subtraction of the fraction of the HK flux which originates in the photosphere leaves a purely chromospheric component, which in the solar case at least is closely related to the surface magnetic flux. In the Appendix we show that for the Sun the integrated emission intensity inside the K1 minima of the K line profile closely approximates the total net radiative loss in

<sup>4</sup> Some of the stars in Figure 1 and Table 1, all labeled "old," do not appear in Vaughan's (1980) study; their classification as old is unambiguous. HD 201091 and 201092, labeled "young" by Vaughan, are here labeled "old" on the basis of their clear activity cycles (cf. Vaughan 1980) and their low absolute emission levels; see also Skumanich and Eddy (1981).

TABLE 1  
DATA AND DERIVED PROPERTIES FOR WILSON SURVEY STARS

Star	S <sub>p</sub>	B-V	<S>	-Log<R <sub>HK</sub> >	-Log<R <sub>HK</sub> >	P <sub>obs</sub> (days)	P <sub>calc</sub> (days)	Old/Young	Star	S <sub>p</sub>	B-V	<S>	-Log<R <sub>HK</sub> >	-Log<R <sub>HK</sub> >	P <sub>obs</sub> (days)	P <sub>calc</sub> (days)	Old/Young
Sun	G2	0.66	0.171	4.614	4.937	25.4	24.8	0	114710	G1	0.58	0.200	4.484	4.756	12.4	12.2	Y
1835	G2	0.66	0.360	4.291	4.415	7.7	6.7	Y	115383	F8	0.58	0.310	4.294	4.449	4.9	4.9	Y
2464	F2	0.43	0.170	4.482	4.793	3.1	3.1	Y	116404	X3	0.93	0.550	4.434	4.467	18.8	15.1	Y
3229	F2	0.44	0.215	4.384	4.612	2.4	2.4	Y	115617*	G6	0.71	0.160	4.689	5.015	32.7	32.7	O
3443	F5	0.74	0.182	4.564	4.917	32.6	32.6	Y	120136	F7	0.48	0.185	4.466	4.759	5.2	5.2	Y
3651	K0	0.85	0.185	4.793	4.960	48.0	42.3	O	124570	F6	0.54	0.135	4.632	5.137	13.9	13.9	O
3785	G3	0.70	0.158	4.985	5.024	31.8	31.8	Y	124850	F7	0.52	0.208	4.434	4.689	6.7	6.7	Y
4628	K4	0.88	0.230	4.740	4.852	38.0	38.6	O	126053	G3	0.63	0.170	4.593	4.930	21.1	21.1	O
6920	F8	0.60	0.190	4.520	4.811	13.1	15.3	Y	131156B	G8	0.76	0.450	4.294	4.375	6.2	7.7	Y
9562	G2	0.65	0.145	4.577	5.102	27.5	27.5	Y	131156B	K4	1.17	1.400	4.417	4.418	11.5	13.2	Y
10476	K1	0.84	0.210	4.724	4.874	38.0	38.0	O	136202	F8	0.54	0.140	4.616	5.089	13.3	13.3	O
10700	G8	0.72	0.172	4.668	4.955	31.9	31.9	O	141004	G0	0.60	0.160	4.595	4.971	18.0	18.5	O
12235	G1	0.62	0.170	4.584	4.924	19.9	19.9	O	142373	F9	0.57	0.142	4.627	5.089	16.8	16.8	O
13421	F8	0.56	0.130	4.559	5.205	17.4	17.4	O	143761	G2	0.60	0.150	4.623	5.041	19.7	19.7	O
16160	K4	0.97	0.230	4.874	4.939	45.0	45.1	O	149661	K0	0.81	0.360	4.451	4.541	21.3	17.7	Y
16673	F6	0.52	0.215	4.419	4.663	5.7	6.3	Y	152391	G8	0.76	0.400	4.345	4.438	11.1	10.5	Y
17925	K0	0.87	0.700	4.242	4.278	6.6	5.2	Y	154417	F8	0.57	0.275	4.340	4.519	7.6	6.1	Y
18256	F5	0.43	0.170	4.482	4.793	3.1	3.1	Y	155885	K1	0.86	0.375	4.500	4.571	22.9	20.9	Y
20630	G2	0.68	0.345	4.327	4.454	9.4	8.7	Y	155885	K1	0.86	0.405	4.466	4.532	20.3	18.3	Y
22049	K2	0.88	0.510	4.394	4.441	11.3	13.0	Y	156026	K5	1.16	0.835	4.624	4.627	18.0	28.2	Y
22072*	G7	0.89	0.135	4.985	5.186	54.1	54.1	O	157856	F5	0.46	0.196	4.433	4.698	3.7	3.7	Y
23249	K0IV	0.92	0.137	5.023	5.186	55.3	55.3	O	158614*	G8IV	0.72	0.165	4.686	4.999	33.0	33.0	O
25998	F7	0.54	0.275	4.323	4.502	2.6	4.5	Y	159332	F4	0.48	0.145	4.572	4.999	7.1	7.1	O
26913	G3	0.70	0.385	4.298	4.407	7.2	7.6	Y	160346	K3	0.96	0.305	4.736	4.787	33.5	37.0	O
26923	G0	0.57	0.285	4.324	4.496	4.07	5.6	Y	161239	G6	0.65	0.140	4.692	5.144	28.5	28.5	O
26965	K1	0.82	0.205	4.708	4.876	37.0	37.0	O	165341A	K0	0.86	0.385	4.488	4.557	19.7	20.0	Y
29645	G3	0.57	0.135	4.549	5.156	17.8	17.8	O	165341B	K5	1.16	0.980	4.555	4.557	22.9	22.9	Y
30495	G1	0.61	0.285	4.352	4.522	7.6	8.0	Y	166620	K2	0.87	0.205	4.776	4.910	42.0	41.0	O
32147	K5	1.07	0.300	4.919	4.940	46.8	46.8	O	176051*	G0	0.61	0.180	4.552	4.865	17.5	17.5	O
33608	F5	0.46	0.210	4.403	4.644	3.3	3.3	Y	176095	F5	0.46	0.200	4.424	4.682	3.6	3.6	O
35296	F8	0.54	0.308	4.273	4.429	3.3	3.3	Y	182101	F6	0.45	0.210	4.399	4.637	2.9	2.9	Y
39587	G0	0.59	0.300	4.315	4.476	5.2	5.9	Y	182572*	G8IV	0.78	0.160	4.766	5.034	40.4	40.4	O
43587	F3	0.61	0.158	4.608	4.990	20.0	20.0	Y	187013	F8	0.46	0.150	4.549	5.4	5.4	O	
45067	F8	0.56	0.140	4.627	5.101	15.8	15.8	O	187691	F8	0.56	0.150	4.597	5.017	14.6	14.6	O
75332	F7	0.42	0.270	4.277	4.443	1.0	1.0	Y	188512*	G8IV	0.86	0.141	4.924	5.148	50.7	50.7	O
76151	G3	0.67	0.260	4.440	4.622	15.0	15.0	Y	190007	K4	1.12	0.780	4.587	4.592	29.3	25.2	Y
76572	F3	0.43	0.146	4.548	4.941	3.8	3.8	Y	190360*	G6IV	0.73	0.155	4.723	5.049	35.9	35.9	O
78366	G0	0.60	0.240	4.419	4.631	10.6	10.6	Y	190406	G1	0.61	0.190	4.528	4.818	13.5	16.4	Y
81809	G2	0.64	0.175	4.588	4.907	21.7	21.7	O	194012	F5	0.51	0.194	4.459	4.739	6.8	6.8	Y
82885	G8IV	0.77	0.315	4.460	4.579	18.1	18.4	Y	201091	K5	1.18	0.605	4.798	4.800	37.9	40.6	O
88737	F5	0.56	0.235	4.402	4.621	7.8	7.8	Y	201092	K7	1.38	0.980	4.909	4.909	48.0	50.0	O
89744	F6	0.53	0.135	4.626	5.130	12.3	12.7	O	206860	G0	0.58	0.323	4.276	4.424	4.7	4.4	Y
97334	G0	0.61	0.320	4.302	4.450	7.6	6.0	Y	207978	F0	0.42	0.155	4.518	4.869	3.1	3.1	O
100180	G0	0.57	0.165	4.562	4.922	14.0	14.4	O	212754	F5	0.52	0.140	4.606	5.075	11.1	11.1	O
100563	F5	0.46	0.195	4.435	4.702	3.8	3.8	Y	216585	F7	0.48	0.141	4.584	5.032	7.3	7.3	O
101501	G8	0.72	0.310	4.412	4.548	17.1	14.5	Y	217014	G5	0.68	0.155	4.674	5.037	29.7	29.7	O
103095	G8	0.75	0.180	4.680	4.930	34.0	34.0	O	219834A	G2	0.79	0.168	4.757	4.999	39.9	39.9	O
106516	F6	0.46	0.208	4.407	4.651	3.4	3.4	Y	219834B	K2	0.91	0.220	4.802	4.902	42.1	42.1	O
107213	F8	0.50	0.138	4.603	5.077	9.2	9.2	O	224930	G2	0.66	0.178	4.596	4.901	23.8	23.8	O
114378	F5	0.45	0.240	4.341	4.541	3.0	2.2	Y									

\* Star not discussed by Wilson 1978, although part of survey.

NOTE ADDED IN PROOF.—For the stars HD 25998 and HD 75332, the values of  $B-V$  used in this table and the figures are significantly discordant with the values of 0.46 and 0.47, respectively, given in the latest edition of the *Yale Bright Star Catalog* (D. Hoffleit 1982, *The Bright Star Catalogue*, 4th rev. ed.; New Haven: Yale University Observatory). These newer values lead to calculated periods  $P_{\text{calc}} = 1.8$  and 2.8 days for the two stars, respectively. We note that for HD 25998, whose period has been observed, the new value of  $P_{\text{calc}}$  is significantly closer to the observed period than is the value given in this table.

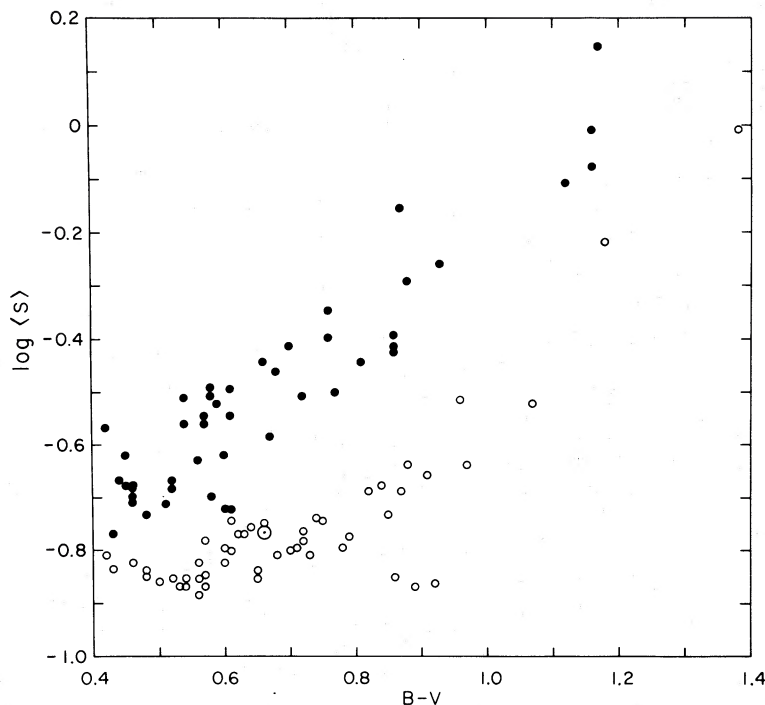


FIG. 1.—Mean values  $\langle S \rangle$  of the Mount Wilson H-K flux index as determined from the long-term survey data of Wilson (1978). In this and the following figure, closed and open circles represent “young” and “old” stars, respectively (Vaughan 1980); the symbol  $\odot$  represents the Sun.

the K line above the temperature minimum. We have therefore determined the total flux passed by the H-K photometer *outside* the K1 and H1 profile minima for the Sun and several other chromospherically weak stars, normalized by the stellar bolometric luminosity. We denote this quantity  $R_{\text{phot}}$  to indicate its photospheric origin and set the true chromospheric emission ratio equal to  $R'_{\text{HK}}$ , where  $R'_{\text{HK}} = R_{\text{HK}} - R_{\text{phot}}$ . We have determined  $R_{\text{phot}}$  from K line profiles of six lower main-sequence stars, and we have fitted a cubic equation to these values to obtain an analytical form for  $\log R_{\text{phot}}$  as a function of  $B-V$ . We explicitly assume that  $R_{\text{phot}}$  depends only on  $B-V$ , independent of chromospheric activity, so that the same value of  $R_{\text{phot}}$  is subtracted from  $R_{\text{HK}}$  for all stars of the same spectral type. This assumption is not strictly true, since the intensity of the solar H and K line wings does increase slightly in solar active regions (White and Livingston 1981); however, the increase in the wings is very much less than that in the line cores, so the approximation is reasonable. The functional relation for  $R_{\text{phot}}$  as a function of  $(B-V)$  is given in the Appendix.

The values of  $\langle R'_{\text{HK}} \rangle$  for the stars under consideration are listed in the sixth column of Table 1 and are plotted versus  $B-V$  in Figure 2. These values are now the basic activity indicator, whose dependence on rotation and convection we shall discuss in § III. Numerically, the values give the fraction of each star's bolometric luminosity which is emitted from the chromosphere (that is, above the temperature minimum) in the Ca II H and K lines.

#### b) Rotation Periods

Rotation periods have been measured for a number of the stars in Table 1, inferred from the period of modulation of the flux index  $S$  in stars monitored at Mount Wilson (Vaughan

*et al.* 1981; Baliunas *et al.* 1983). These are listed in the seventh column of Table 1. In addition to the periods reported in the above two references, several new rotation periods are reported here for the first time. The observational data for these stars are listed in Table 2, and the periods derived are also entered in the seventh column of Table 1. (For description of the method of period determination and the meaning of the significance parameters  $\Sigma_{\text{peak}}$ , see Baliunas *et al.* 1983). Finally, the period of the star HD 39587 is taken from the work of Stimets and Giles (1980), who extracted it from the long-term survey data of Wilson (1978). Observed rotation periods, rounded to the nearest day, are shown next to the corresponding data points in Figure 2.

#### c) Properties Depending on Spectral Type

In this paper we shall use the  $B-V$  color index to specify the main-sequence spectral type and relevant convective properties which depend on spectral type. Specifically, in § III below we shall consider theoretical convective overturn times, which have been calculated for lower main-sequence stars as a function of mass. We relate mass to  $B-V$  color index through

$$\log (M/M_{\odot}) = 0.28 - 0.42(B-V). \quad (1)$$

This relation is taken from data tabulated by Allen (1973) and fits these data to  $\pm 0.01$  in  $\log M/M_{\odot}$  for  $0.4 < B-V < 1.4$ . We shall also have occasion to evaluate the effective temperature  $T_{\text{eff}}(B-V)$ . From tabulated data in Johnson (1966), we find

$$\log T_{\text{eff}} = 3.908 - 0.234(B-V), \quad (2)$$

which fits those data to about  $\pm 0.002$  in the range  $0.4 < B-V < 1.4$ .

The values of  $B-V$  listed in Table 1 are from Vaughan (1980).

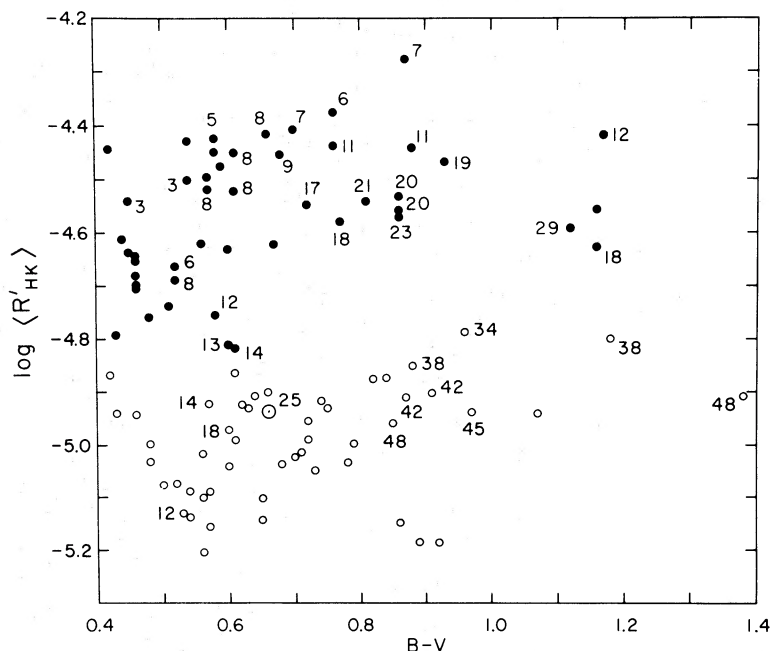


FIG. 2.—The mean chromospheric H-K flux ratio  $\langle R'_{HK} \rangle$ , as obtained from the mean Wilson (1978) survey data plotted in Fig. 1. Labels give observed periods in days of the measured stars from the seventh column of Table 1.

### III. ANALYSIS

In Figure 3 we plot  $\langle R'_{HK} \rangle$  versus rotation period for the stars in Table 1 for which periods have been measured. The points are labeled by their  $(B-V)$  color index. Although a general correlation is apparent, in that  $\langle R'_{HK} \rangle$  decreases with increasing rotation period, there is considerable scatter in this correlation. This scatter exhibits a dependence on color, in the

TABLE 2  
RECENTLY DERIVED ROTATION PERIODS FROM THE H-K PROGRAM

Star Name	HD Number	$P \pm d_p^a$ (days)	$\Sigma_{\text{peak}}^b$	Max Lag <sup>c</sup> (days)	$N_{\text{peak}}^d$
11 LMi.....	82885	$18.1 \pm 0.1$	8.8	120	6
42 Leo.....	89744	$12.3 \pm 0.3$	3.0	60	3
	95735	48	2	90	1
	97334	$7.6 \pm 0.1$	4.1	70	5
88 Leo.....	100180	14	2.6	40	1
61 UMa.....	101501	$17.1 \pm 0.4$	3.6	80	2
(42)Com.....	114378	$3.0 \pm 0.1$	2.6	40	2
(43)Com.....	114710	$12.4 \pm 0.2$	4.0	90	4
	115404	$18.8 \pm 0.1$	7.6	100	5
	124850	$7.6 \pm 0.6$	1.8	70	2
(37)Boo.....	131156A	$6.2 \pm 0.1$	4.9	100	5
(37)Boo.....	131156B	$11.5 \pm 0.2$	4.0	100	5
$\lambda(27)$ Ser.....	141004	18	2	70	1
70 Oph.....	165341A	$19.7 \pm 0.1$	7.2	90	3

<sup>a</sup> The measured period  $P$  is determined from the average (if more than one peak is observed) of the position of the autocorrelation peak divided by the peak number.  $d_p$  is the standard deviation of  $P$  and represents the precision of  $P$ .

<sup>b</sup> The combined significance of the height of the peaks of the autocorrelation coefficients.

<sup>c</sup> Maximum lag over which the autocorrelation is calculated.

<sup>d</sup> The number of peaks in the autocorrelation analysis that were used to determine the period.

sense that stars with smaller  $(B-V)$  appear to be displaced either downward or to the left with respect to stars with larger  $(B-V)$ . Such a color-dependent scatter could result from one of two possibilities, or a combination of the two. The first alternative is that  $\langle R'_{HK} \rangle$ , the ordinate of Figure 3, is an inappropriate parameter because it fails to include some color-dependent quantity which would raise earlier spectral types in the diagram with respect to later spectral types and thus decrease the scatter. For example, instead of the chromospheric flux ratio  $R'_{HK}$  we may consider the surface flux itself,  $F'_{HK} = R'_{HK} \times \sigma T_{\text{eff}}^4$ . As Figure 4 shows, plotting  $F'_{HK}$  rather than  $R'_{HK}$  versus  $P_{\text{obs}}$  decreases the scatter significantly, because the factor  $\sigma T_{\text{eff}}^4$  elevates earlier spectral types more than later spectral types in the diagram. [We have used  $\log(\sigma T_{\text{eff}}^4) = 11.386 - 0.937(B-V)$  from eq. (2)]. The reasonably small dispersion of points about a mean trend in Figure 4 is in basic agreement with the results of Catalano and Marilli (1983) and Middelkoop (1982).

However, there is a second possible cause of the color-dependent dispersion of points in Figure 3, and as we shall see below, allowing for this possibility produces an even smaller scatter than is seen in Figure 4. This alternative is that  $P_{\text{obs}}$ , the abscissa of Figure 3, is an inappropriate parameter because it fails to include some color-dependent quantity which would translate earlier spectral types to the right with respect to later spectral types, and thus decrease the scatter. On physical grounds, we might expect the chromospheric emission ratio  $R'_{HK}$  to depend on both rotation period  $P_{\text{obs}}$  and spectral type if convection zone properties have an effect on magnetic field generation.

An important parameter of hydromagnetic dynamo theory, which depends on both rotation rate and spectral type, is the Rossby number  $Ro$ . This dimensionless number is the ratio of the stellar rotation period  $P$  to the convective turnover time

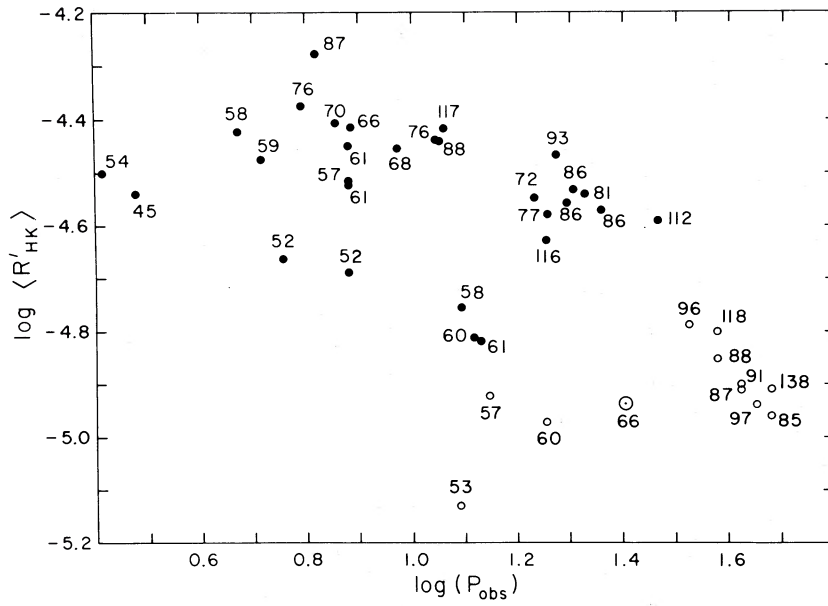


FIG. 3.—Variation of the mean chromospheric H-K flux ratio  $\langle R'_{HK} \rangle$  with observed rotation  $P_{obs}$ , for stars whose rotation period has been measured by rotational modulation of Ca II K (seventh column of Table 1). Labels give  $100(B-V)$ .

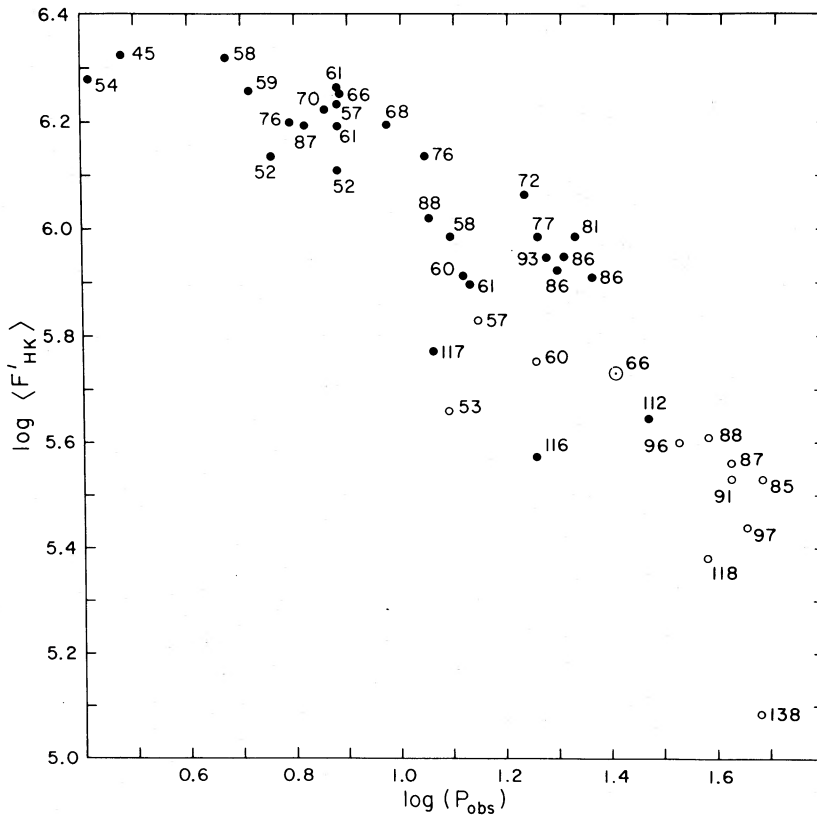


FIG. 4.—The mean chromospheric flux  $\langle F'_{HK} \rangle = \sigma T_{eff}^4 \langle R'_{HK} \rangle$  vs. rotation period  $P_{obs}$ . Labels give  $100(B-V)$

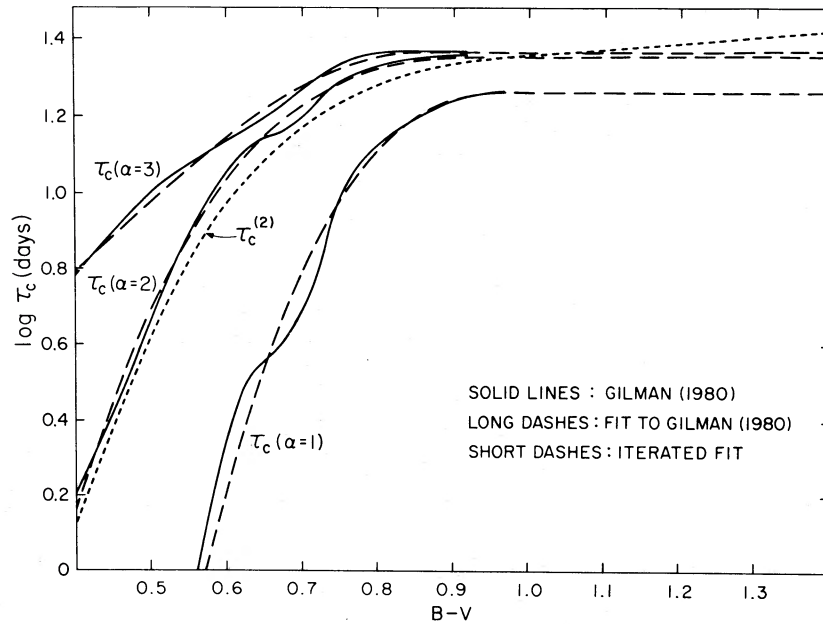


FIG. 5.—Solid Lines: Convective overturn time  $\tau_c$  according to calculations of Gilman (1980) for convection zone models with  $\alpha = 1, 2,$  and  $3$ . Long dashed lines: Numerical fits to Gilman's calculations. Short dashed lines: Iterated function  $\tau_c^{(2)}$ , given by eq. (4).

$\tau_c$  in that part of the convection zone where dynamo activity is situated. It is a measure of the importance of coriolis forces in introducing helicity into convective motions.

Dynamo generation of magnetic fields is more commonly parameterized by the dynamo number  $N_D$ , which is essentially the ratio between magnetic field generation and diffusion terms in the convection zone. In very general terms, it may be written (Parker 1979)  $N_D = \alpha \Omega d^4 / \eta^2$ . In this equation,  $\alpha$  is the product of the mean helicity of convection  $\langle \mathbf{v} \cdot (\nabla \times \mathbf{v}) \rangle$  and the characteristic convective turnover time  $\tau_c$ ,  $\Omega'$  is the depth gradient of the angular rotation  $\Omega$ ,  $d$  is the characteristic length scale of the convection, and  $\eta$  is a turbulent magnetic diffusivity, which scales like  $d^2 / \tau_c$ . If we note that  $\alpha$  scales like  $\Omega d$ , and make the reasonable assumption that  $\Omega'$  scales like  $\Omega / d$ , we find that  $N_D \approx (\Omega \tau_c)^2 = \text{Ro}^{-2}$ . Precisely this relationship between dynamo number and Rossby number has previously been suggested by Durney and Latour (1978).

The above relation  $N_D \sim \text{Ro}^{-2}$  depends essentially on dimensional analysis. The precise way in which the Rossby number enters the physics of dynamo field generation is undoubtedly more complex, and its specification is heavily model-dependent. Nevertheless, it is to be expected that, qualitatively at least, magnetic activity should increase with decreasing Rossby number  $\text{Ro}$ , and therefore it seems appropriate to see if an empirical correlation does in fact exist between chromospheric emission and this simple dimensionless parameter.

In order to explore how the chromospheric emission ratio  $R'_{\text{HK}}$  depends on  $\text{Ro}$  we shall set  $\text{Ro} = P_{\text{obs}} / \tau_c$ , where  $P_{\text{obs}}$  is the observed rotation period from the seventh column of Table 1, and  $\tau_c$  is the convective turnover time as given by Gilman (1980). The data presented by Gilman were calculated using a convection code developed by J. Latour; the physics of the code is very similar to that used by Baker and Temesvary (1966).

One rather ill-defined parameter that occurs in the convection zone models, and which significantly affects the calculated convective turnover time, is  $\alpha$ , the ratio of mixing length to scale height. Since its actual value is not well determined, in this paper models were examined within a family of values of  $\alpha$ . Following Gilman, we have considered the functions  $\tau_c(B-V)$  for the three values  $\alpha = 1, 2,$  and  $3$ . These functions are replotted from Gilman's work in Figure 5, along with a cubic fit to each for ease of subsequent computation. Gilman's calculations did not extend to  $(B-V) > 0.9$ ; for our present purpose we simply assumed  $\tau_c$  constant for  $B-V > 0.9$ . We note that for  $(B-V) < 0.9$ ,  $\tau_c$  increases with advancing spectral type, rather steeply at earlier spectral types and less steeply at later spectral types. Also,  $\tau_c$  is larger for convection zone models with larger  $\alpha$ . This is because models with larger  $\alpha$  have deeper convection zones, and therefore higher densities, lower convective velocities, and larger scale heights near the bottom of the convection zone. In addition, Figure 5 shows that  $\log \tau_c$  increases more slowly with advancing spectral type for larger values of  $\alpha$ . This  $\alpha$ -dependence of the functional form of  $\tau_c(B-V)$  produces a corresponding  $\alpha$ -dependence in the run of Rossby number with  $B-V$ , for a given rotation period.

In Figure 6 we plot, for stars with measured rotation periods, the observed chromospheric emission ratio  $\langle R'_{\text{HK}} \rangle$  versus Rossby number, assuming  $\alpha = 1$  and  $2$ . We used the smooth dashed curves in Figure 5 to define the run of  $\tau_c$  with  $B-V$ , rather than the actual results of Gilman's calculation (solid lines in Fig. 5), because the small-scale irregularities of the latter are not considered significant (P. Gilman, personal communication). We see from Figure 6b that the scatter from a smooth relationship is quite small for the case  $\alpha = 2$ . In particular, it is very much less than the scatter in the relation between  $\langle R'_{\text{HK}} \rangle$  and  $P_{\text{obs}}$  alone (Fig. 3). This is because the earlier spectral types, which tend to lie in the lower left of Figure 3, have been displaced to the right relative to later

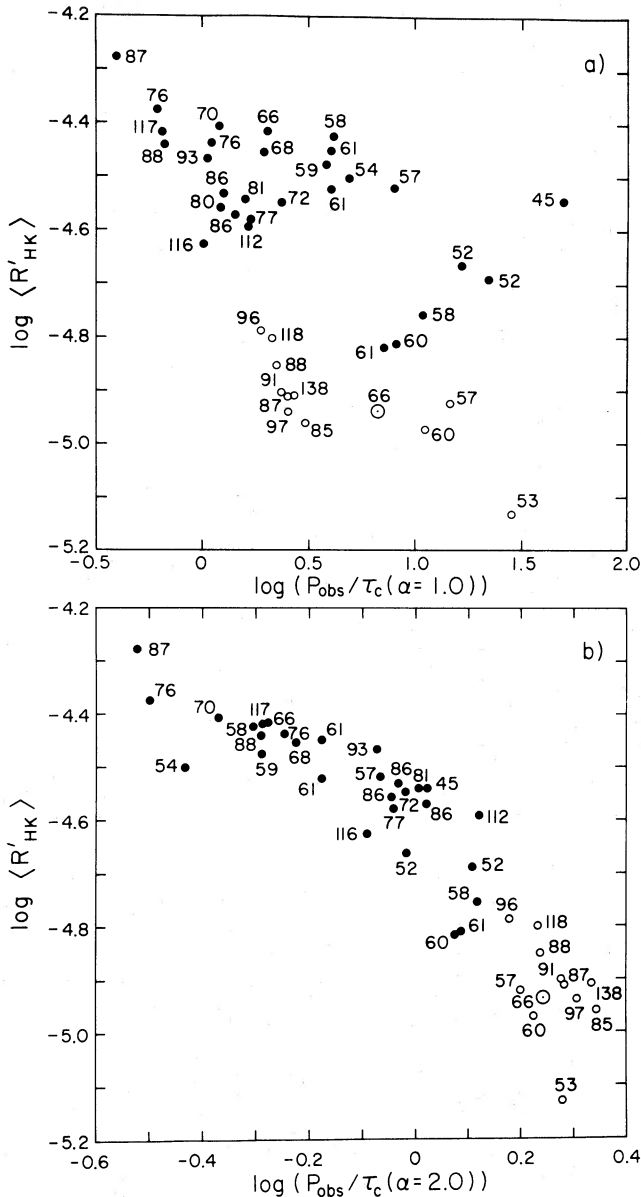


FIG. 6.— $\langle R'_{\text{HK}} \rangle$  plotted vs. the Rossby number  $P_{\text{obs}}/\tau_c$  (a) for  $\alpha = 1$  and (b) for  $\alpha = 2$ . In each case the convective overturn time  $\tau_c$  is given as a function of  $(B-V)$  by the appropriately labeled long dashed line in Fig. 5.

type stars, owing to the smaller convective overturn time of the earlier type stars. The scatter in Figure 6 also is somewhat smaller than in the plot of  $\langle F'_{\text{HK}} \rangle$  versus  $P_{\text{obs}}$  (Fig. 4). Although here the improvement is not so striking, it is unambiguous: the mean scatter in  $|\log R'_{\text{HK}}|$  of the points in Figure 6b from a smooth curve passing through the data is about 0.06 dex, while the mean scatter in  $|\log F'_{\text{HK}}|$  of the points in Figure 4 from a smooth curve passing through these data is about 0.11 dex.

We note, however, that the small scatter in the plot of  $\log R'_{\text{HK}}$  versus Rossby number is achieved only for a particular choice of the parameter  $\alpha$ , namely  $\alpha = 2$  (Fig. 6b). When the data are plotted versus Rossby number calculated for  $\alpha = 1$

(Fig. 6a) the scatter is very much larger. It is also slightly larger for the case  $\alpha = 3$  (not shown) than for  $\alpha = 2$ .

We have made plots similar to those of Figure 6 for intermediate values of  $\alpha$ , using functions  $\tau_c(B-V)$  obtained by quadratic interpolation between the dashed curves of Figure 5, and found a minimum dispersion of points from a smooth curve for  $\alpha \sim 1.9$ . For computational purposes only, we placed a cubic fit through the data for  $\alpha = 1.9$ , given by

$$\log (P/\tau) \equiv f(\langle R'_{\text{HK}} \rangle) = 0.324 - 0.400y - 0.283y^2 - 1.325y^3, \quad (3)$$

where  $y = \log (10^5 R'_{\text{HK}})$ . We then subtracted  $f(\langle R'_{\text{HK}} \rangle)$  from  $\log P_{\text{obs}}$  and plotted the resulting points versus  $B-V$  (Fig. 7). A cubic fit through these points (solid line) then defines an empirical iterated function  $\log \tau_c^{(2)}(B-V)$ , given by:

$$\log \tau_c^{(2)} = \begin{cases} 1.362 - 0.166x + 0.025x^2 - 5.323x^3, & x > 0 \\ 1.362 - 0.14x, & x < 0 \end{cases} \quad (4)$$

where  $x = 1 - (B-V)$ . This curve is also reproduced as a dashed line in Figure 5. It differs only slightly from the interpolated theoretical curve for  $\alpha = 1.9$ , except for the fact that we have allowed  $\tau_c^{(2)}$  to increase slightly with increasing  $(B-V)$  past the limit of  $B-V \sim 0.9$  in Gilman's calculations. (Such an increase would be expected theoretically, although we did not include it in the initial functions of Fig. 5. Unfortunately, as may be seen in Fig. 7, there are few data points presently available for  $B-V > 1.0$ , so the actual trend of  $\tau_c^{(2)}$  in this region is poorly defined.)

Figure 8 shows the observed values of  $\langle R'_{\text{HK}} \rangle$  plotted versus  $P_{\text{obs}}/\tau_c^{(2)}$ ; the dispersion is only slightly decreased over the initial diagram for  $\alpha = 1.9$ , and we therefore did not carry the iteration further. The solid line in Figure 8 is equation (3). We attach no physical significance to its functional form, which was derived simply as a numerical aid to the iteration. However, in § IV below we shall discuss some possible interpretations of the general trend of the data in Figure 8.

#### IV. DISCUSSION

##### a) Implications for Stellar Convection and Dynamos

The data shown in Figure 6b and 8 suggest that the mean level of chromospheric activity in lower main-sequence stars is governed to a large extent by the single parameter  $P/\tau_c$ , where  $\tau_c$  is an empirical function of  $B-V$  very similar to the theoretically calculated convective overturn time (see Fig. 5). This gives strong support to the idea that the ratio of rotation period to convective overturn time, or the Rossby number  $Ro$ , is in fact a major determinant of magnetic field amplification in convecting and rotating stars. As we have mentioned, such an idea is implicit in standard  $\alpha$ - $\omega$  dynamo theory.

The tightness of the relation shown in Figures 6b and 8 is actually somewhat surprising, even if there is a unique relation between dynamo field generation and Rossby number. What is observed, of course, is not the fields generated in the deep convection zone but the chromospheric emission resulting from heating associated with surface fields. The rise of dynamo-generated field to the surface, its stressing by convective motions near the surface, the propagation of these stresses upward into the chromosphere, the release of the stresses in chromospheric heating, and the resulting production of H-K

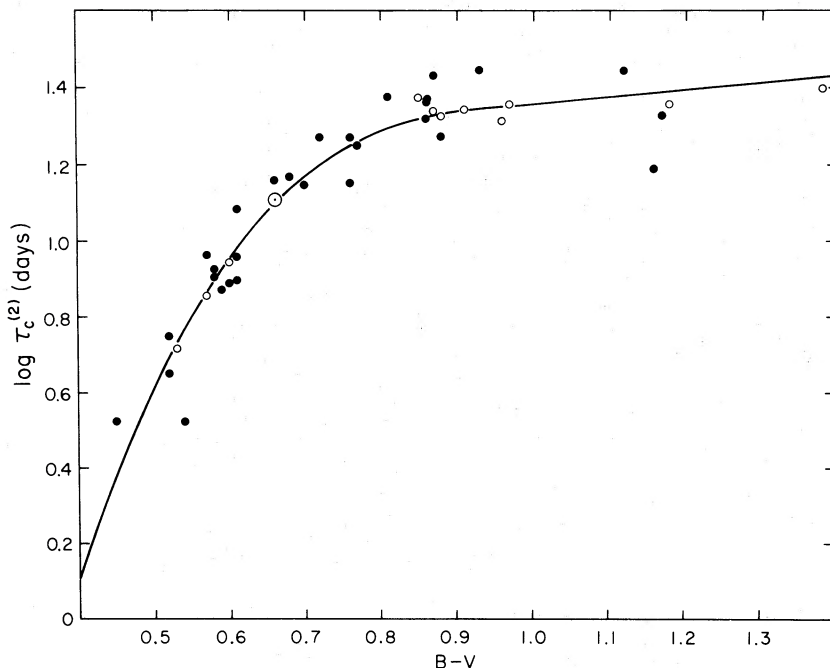


FIG. 7.—The quantity  $\log \tau_c^{(2)} = \log P_{\text{obs}} - f(\langle R'_{\text{HK}} \rangle)$ , plotted vs.  $(B-V)$  where  $f(\langle R'_{\text{HK}} \rangle)$  is given by eq. (3). Solid line is eq. (4).

emission together constitute a complex transfer mechanism. That this transfer mechanism should be essentially independent of spectral type is scarcely to be anticipated. The implication of the present results that this in fact may be the case could provide useful clues about the nature of the mechanism.

The detailed relation between  $R'_{\text{HK}}$  and  $P/\tau_c$ , given by the trend of the data points in Figure 8, in principle should give quantitative information on the dependence of dynamo activity

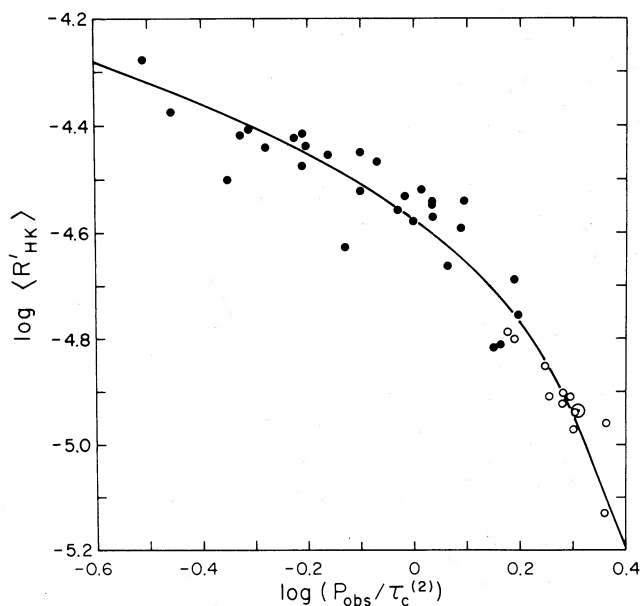


FIG. 8.— $\langle R'_{\text{HK}} \rangle$  plotted vs.  $P_{\text{obs}}/\tau_c^{(2)}$ , where  $\tau_c^{(2)}$  is given by eq. (4). Solid line is eq. (3).

on Rossby number. Unfortunately, the physical interpretation of the relationship is far from clear. The data trend in Figure 8 indicates a smooth increase of  $R'_{\text{HK}}$  with decreasing Rossby number or equivalently increasing dynamo number. The rate of increase is large for large Rossby number and becomes less for small Rossby number. A possible reason for this could be negative feedback produced by large magnetic fields in the convection zone, acting to reduce the  $\alpha$ -effect dynamo and differential rotation, as suggested by Robinson and Durney (1982). An alternative, less physically interesting reason, however, might be found in a saturation of H-K emission in regions of high magnetic flux. (The emission, of course, can never exceed the Planck function characteristic of the temperature of formation of Ca II.) A third possibility arises from recent findings that on chromospherically active, rapidly rotating G and K dwarfs, spot areas are much larger than on less active stars like the Sun (Chugainov 1980; Radick *et al.* 1982). If, as for the Sun, chromospheric emission from spots is not increased in proportion to the magnetic flux increase in spots over that in plages (in the Sun it actually decreases in spots), and if in the more rapidly rotating dwarfs a larger fraction of the total magnetic flux occurs in spots, the H-K emission ratio from the star as a whole could approach saturation with increasing dynamo activity even if the total magnetic flux did not. Finally, it may be noted that the data of Figure 8 could also be fit by an exponential relation, of the form  $R'_{\text{HK}} \sim 6 \times 10^{-5} \exp(-0.9P/\tau_c^{(2)})$ . The data by themselves are not sufficient to determine a clearly preferable functional relation between  $R'_{\text{HK}}$  and Rossby number.

In order to use the shape of the curve in Figure 8 as a guide to the mechanism of stellar dynamos, certain supplementary information would be required. Most important, of course, is knowledge of the detailed relation between Ca II emission ratios and underlying photospheric magnetic flux, for stars of

different spectral types and rotation rates. In addition, other information such as spot area coverage, or surface brightness and area coverage of chromospheric active regions, would be very helpful. Such information may be obtainable from photometric and spectrophotometric (HK) rotational modulation light curves.

Turning to the detailed dependence of  $\tau_c$  on  $B-V$ , we note that the empirical function  $\tau_c^{(2)}(B-V)$  closely matches the theoretical convective overturn time for  $\alpha \sim 2$  (Fig. 5). As mentioned above, the scatter in plots of  $\log \langle R'_{\text{HK}} \rangle$  versus  $P/\tau$  is slightly greater for  $\alpha = 3$  than for  $\alpha = 2$ , and very much greater for  $\alpha = 1$ . To the extent that the various assumptions made in the analysis are valid, this would suggest that  $\alpha \sim 2$  is a better description of convective envelopes of lower main sequence stars than  $\alpha \sim 1$  or (with somewhat less confidence)  $\alpha \sim 3$ . A ratio of mixing length to scale height  $\alpha \sim 2$  implies a deeper convection zone than for the case  $\alpha \sim 1$ ; for the Sun, for example, the models of Gilman (1980) yield convection zone depths of 26% and 15% of the radius for  $\alpha = 2$  and  $\alpha = 1$ , respectively. We may note that solar models with  $\alpha \sim 2$  provide good agreement between stellar evolution calculations and the known physical parameters of the present-day Sun (Gehren 1982). In addition, results emerging from studies of the solar  $p$ -mode oscillations (helioseismology) suggest that the solar convection zone may be significantly deeper than predicted by models with  $\alpha = 1$  (Lubow, Rhodes, and Ulrich 1980; Berthomieu *et al.* 1980). Also, Gilman (1980) finds that his numerical calculations of convection in the rotating Sun cannot produce surface differential rotation in agreement with observations (angular velocity increasing monotonically from pole to equator) unless  $\alpha > 2$ .

While we consider the agreement between our "best fit" value of  $\alpha$  and independent assessment of  $\alpha$  to be encouraging, we stress that it is inappropriate to use the present results to infer the value of  $\alpha$ . There are a number of reasons for our caution:

1. Different series of interior models may give slightly different functional shapes of  $\tau_c(B-V)$  for the same value of  $\alpha$ . We have not carried out a detailed comparison of different interior models in this investigation.

2. We have assumed, following Gilman (1980) that dynamo activity is situated one pressure scale height above the bottom of the convection zone. If this assumption is changed, the calculated function  $\tau_c(B-V)$  will change correspondingly. For example, if the stars under study have even deeper convection zones, corresponding to  $\alpha \gtrsim 3$ , but if at the same time their dynamo activity is situated further above the convection zone base, specifically at the same location calculated by Gilman for the  $\alpha \sim 2$  models, then the variation of convective overturn time with  $B-V$  will be rather similar to that for the present  $\alpha = 2$  calculation. (Conversely, given the above-mentioned independent evidence that  $\alpha \sim 2$  does describe convection zones well, then the present results would support the idea that dynamo activity occurs near the base of the convection zone.)

3. As stated earlier, there is no *a priori* reason to expect the chromospheric emission ratio  $R'_{\text{HK}}$  to respond to the dynamo process in a way independent of spectral type. A smooth variation with spectral type of the chromospheric response to dynamo-generated magnetic fields could cause the scatter in  $R'$  versus  $P/\tau_c$  to be minimized at an incorrect value of  $\alpha$ .

4. As we have mentioned, the conjecture that dynamo activity is a function of the single parameter  $\text{Ro} = P_{\text{rot}}/\tau_c$  is based on the assumption that differential rotation, which is critical to dynamo operation, scales with rotation itself. While rotation itself is likely to be the dominant determinant of differential rotation, other effects dependent on spectral type could enter and give a slightly different dependence of magnetic activity on convection and rotation. For example, Durney and Robinson (1982) argue that dynamo activity may depend, not on  $\text{Ro}$  alone, but on  $\text{Ro}(H/r_c)^{1/2}$ , where  $H$  is the pressure scale height at the base of the convection zone and  $r_c$  is the radius of the base of the convection zone. Plots of  $R'_{\text{HK}}$  versus  $\text{Ro}(H/r_c)^{1/2}$  yield minimal scatter for a slightly smaller assumed value of  $\alpha$  than that which minimizes the scatter in  $R'_{\text{HK}}$  versus  $\text{Ro}$  alone. Durney and Robinson state that it is not clear on intuitive grounds which of the two assumptions is to be preferred, and that further research is needed. [The present data actually would appear to support the assumption of dynamo dependence on  $\text{Ro}$  alone rather than on  $\text{Ro}(H/r_c)^{1/2}$ , because the minimized scatter is somewhat less under the first assumption. However, the above-mentioned uncertainty in our knowledge of the relation between  $R'_{\text{HK}}$  and actual surface magnetic activity prevents our validating the first assumption solely on that basis.

To take the point one step further, we cannot rule out the possibility that a spectral-type dependence of the conversion between dynamo-generated magnetic fields and chromospheric heating, plus errors introduced in converting from measured HK flux index  $S$  to chromospheric emission ratio  $R'_{\text{HK}}$  (see the Appendix), plus an incorrect choice of the function  $P/\tau_c^{(2)}$  to parameterize dynamo activity, all have conspired to minimize the scatter in Figures 6b and 8. Therefore, the smallness of the scatter does not allow us to rule out the suggestion (Catalano and Marilli 1983; Middelkoop 1982) that the true independent parameter controlling magnetic field generation is the rotation period itself, as might be indicated by Figure 4. However, in view of the facts that (a) the dimensionless ratio of rotation period to convective turnover time is a more natural parameter of dynamo theory than the period itself, and (b) the empirical function  $\tau_c(B-V)$  which minimizes the dispersion of  $\langle R'_{\text{HK}} \rangle$  versus  $P_{\text{obs}}/\tau_c$  is close to the theoretically calculated convective turnover time for a plausible value of  $\alpha$ , we suggest that the interpretation we have advanced is a more reasonable one.

To summarize, it is very suggestive that the chromospheric emission ratio  $R'_{\text{HK}}$  seems to be a tight function of  $\text{Ro} = P/\tau_c$ , with  $\tau_c$  evaluated near the bottom of the convection zone for convection zone models with  $\alpha \sim 2$ . However, we will require additional independent information, such as the most appropriate value of  $\alpha$  (e.g., through helioseismology), or the relation between  $R'_{\text{HK}}$  and surface magnetic flux for different spectral classes and activity levels, before the observational results presented here can provide a unique specification of the dependence of magnetic activity on rotation and convection.

#### b) Implications for the Vaughan-Preston Gap

As may be seen from the data plotted in Figure 8, there is no indication of a discontinuity in the relation of  $\langle R'_{\text{HK}} \rangle$  to  $P/\tau_c$  between "young" and "old" stars—that is, stars above and below the Vaughan-Preston gap. This is of interest in relation to recent conjectures that the gap may be caused by

a near-discontinuous change of dynamo activity to a less efficient mode at a critical (perhaps mass-dependent) rotation rate. Such a change would cause a star to undergo a sudden decrease of surface activity when its rotation decreases (presumably as a result of stellar wind angular momentum loss) below the critical rate. There would then be a relative paucity of stars with activity slightly below that characteristic of the critical rotation rate. Specifically, Durney, Mihalas, and Robinson (1981) have suggested that such a critical rotation rate separates a regime of higher rotation, where several dynamo modes are excited, from one of lower rotation where only the fundamental mode is excited. Knobloch, Rosner, and Weiss (1981), on the other hand, suggest that above a critical rotation rate convection occurs, not in convective eddies, but rather in longitudinal rolls, and that in the latter case the surface fields might well be amplified to higher values than in the former case.

In such conjectures, it would be expected that  $R'_{\text{HK}}$ , plotted in Figure 8, would show a different dependence on  $P/\tau_c$  for older stars (*open circles*) than for younger stars (*closed circles*); namely, the older stars should lie systematically about 0.2 dex lower than the young stars (the width of the gap; see Fig. 2). This is not the case; Figure 8 suggests that  $R'_{\text{HK}}$  decreases smoothly and continuously as a star's rotation period increases, and it evolves from above to below the gap. Also, Figure 7 indicates that the empirically derived function  $\tau_c^{(2)}$  has approximately the same dependence on  $B-V$ , and the same numerical value, for stars above and below the gap. If stars of a given  $B-V$ , just above and just below the gap, while differing in  $R'_{\text{HK}}$ , had nearly the same rotation period, the derived value of  $\log \tau_c = \log P_{\text{obs}} - f(R'_{\text{HK}})$  would be systematically different for the two classes. Baliunas *et al.* (1983) have also seen no systematic change in the dependence of chromospheric emission upon rotation period for stars above and below the gap, using a smaller subset of the present data.

This result casts doubt on the hypotheses mentioned above, of a sharp drop in dynamo efficiency at a (possibly mass-dependent) rotation rate. It is, however, consistent with three alternative hypotheses:

1. The gap is not real but simply represents a chance fluctuation in the chromospheric activity distribution for stars in the solar neighborhood.
2. The gap is statistically significant and represents a true bimodal distribution of the *ages* of stars in the solar neighborhood. In other words, although rotation rate and as a result chromospheric emission both decrease smoothly with age, there is a relative paucity in the solar neighborhood of stars of that age, and hence rotation rate, which would produce emission levels corresponding to the gap.
3. The gap is real and results from the circumstance that at a critical (possibly mass-dependent) rotation rate there occurred an epoch of rapid spindown, perhaps due to an enhanced stellar wind (see Durney, Mihalas, and Robinson 1981). This would cause  $R'_{\text{HK}}$  to decrease correspondingly if it bears the same relation to period implied by Figure 8 for both fast and slow rotators, and therefore a gap would result in the distribution of chromospheric emission level.

Hypothesis 3 is intriguing, but there is at present no independent evidence supporting such a period of rapid spindown. Soderblom (1983) concludes that the  $v \sin i$  values of field stars do not show a gap at an age corresponding to

that of the Ca II emission gap. This would be consistent with our results only under hypothesis 1. Also, Hartmann *et al.* (1984) have considered the statistical significance of the gap as outlined in the Vaughan and Preston (1980) neighborhood survey and find that it is *not* high, which favors hypothesis 1.

It should be noted that the conclusions we have drawn from Figures 6–8 are in some disagreement with earlier findings. Thus Middelkoop (1982) found, at least for the spectral range  $0.52 < B-V < 0.63$ , that Ca II H and K emission decreases rapidly without a corresponding decrease in rotation rate, at a rotation period of about 12 days, or  $v \sin i \sim 4 \text{ km s}^{-1}$ . The data underlying this conclusion, however, retain the ambiguity of  $\sin i$ ; also Middelkoop noted that the smaller values of  $v \sin i$  entering the analysis (that is, values less than  $2\text{--}2.5 \text{ km s}^{-1}$ ) may be at or below the limit of measurability using line profile analysis. Therefore Middelkoop's result needs confirmation. Duncan (1981), in analyzing lithium ages of field stars, concluded that there was some evidence for a sudden decrease of stellar chromospheric emission at an age  $1\text{--}2 \times 10^9$  years; this would be consistent with the findings in this paper only under hypothesis 3 above.

Finally, we should emphasize that although the present data do not support the idea of a sudden decrease of dynamo efficiency at a particular rotation rate, they are not inconsistent with a change with rotation of the relative importance of different dynamo modes, as suggested by Durney, Mihalas, and Robinson (1981), as long as there is no resulting discontinuous change in activity level. Indeed, the observation by Vaughan *et al.* (1981), that regular cycles appear only for rotation periods longer than about 20 days, supports this conjecture.

### c) *The Use of the Relationship as a Rotation Period Predictor*

The points in Figure 8 exhibit a root mean square deviation in  $\log(P/\tau)$  about the mean curve of about 0.08. This suggests that one may predict stellar rotation periods to comparable accuracy from observed values of mean chromospheric emission ratios  $\langle R'_{\text{HK}} \rangle$ , and  $(B-V)$ , using equations (3) and (4). Values of rotation period predicted in this way are listed in the eighth column of Table 1 for all stars in the long-term Mount Wilson activity survey. (Several of the observed rotation periods listed in the seventh column were in fact successfully predicted in this fashion before the observed periods were obtained.) An earlier but rather similar form of the predictive relation for rotation derived by Noyes (1983) was used by Vaughan (1983) in discussing the relation between stellar rotation periods and activity cycles. The relationship given here is used by Duncan *et al.* (1984) to infer rotation periods for Hyades stars from their HK flux.

We wish to thank J. Frazer, H. Lanning, T. Misch, and J. Mueller for their dedicated efforts in data acquisition, and L. Woodward and J. Horne for data management and processing. We are grateful to Drs. E. Avrett, L. Belsere, P. Gilman, D. Gough, B. Durney, R. Rosner, N. Weiss, and C. Zwaan for useful comments about this work. We wish to acknowledge support of this research in part from NSF grant AST 81-21726, from the Smithsonian Institution Scholarly Studies Program, and from the National Geographic Society grant 2548-82.

## APPENDIX

THE RELATION BETWEEN THE HK FLUX INDEX  $S$  AND CHROMOSPHERIC FLUX RATIO  $R'_{\text{HK}}$ 

The calibration of the Ca II radiative losses is an important aspect of our analysis. The  $S$  index depends not only upon chromospheric radiation, but also on the photospheric emission in the neighboring line wings, which is a rapidly varying function of spectral type. In order to compare the true chromospheric emission of stars with different  $B-V$ , it is necessary to calibrate the variation of the photospheric flux.

a) The Conversion of  $S$  to Flux Ratio  $R_{\text{HK}}$ 

Middelkoop (1982) has estimated the conversion of  $S$  into a quantity  $R_{\text{HK}} \propto F_{\text{HK}}/\sigma T_{\text{eff}}^4$ , where  $F_{\text{HK}}$  is the flux per  $\text{cm}^{-2}$  in the  $H$  and  $K$  bandpasses. This calibration has the advantage that it was derived using the H-K photometer itself, and so the passbands are guaranteed to be correct. Unfortunately, the measurements are not in terms of absolute spectrophotometry, since the H-K photometer is a slit spectrograph instrument. Furthermore, no extinction corrections were performed, although the effects of differential extinction were minimized as far as possible. Therefore, it is important to try to check this calibration using other spectrophotometry.

We used the following procedure. A source of relative spectrophotometry was used to relate the flux in the continuum bandpasses to the flux at 5500 Å. We then assumed that the surface flux at this wavelength was given by the relation of Barnes and Evans (1976) for the surface flux in the  $V$  bandpass. Since Middelkoop derived the correction factor in terms of  $B-V$ , we used the Barnes-Evans relation as a function of  $B-V$  to derive the surface fluxes in the continuum bandpasses. Then using the  $S$  index, which is the ratio of the line center flux to the continuum flux, the value of  $R_{\text{HK}}$  was determined. Note that this method provides a relative, not an absolute, calibration.

O'Connell (1973) presented stellar energy distributions at specific wavelengths in 20 Å bandpasses. Two of the measurement points were made at 3889 and 3910 Å; we assumed that a suitable average of these values could be used to represent the violet continuum bandpass of the HK photometer, which is 20 Å wide centered at 3901 Å. The ratio of fluxes in the red and violet bandpasses is given by the  $C_{rv}$  color tabulated by Vaughan and Preston (1980); we used the mean relationship between  $C_{rv}$  and  $B-V$  to derive the total continuum fluxes from spectrophotometry for the violet bandpass.

A disadvantage of using O'Connell's data is that results are listed for an average of spectral subtypes, e.g., K5-M0. We have assigned  $B-V$  colors and effective temperatures to these mean spectral types following Johnson (1966).

The other source of spectrophotometry used was the data set of Faÿ, Stein, and Warren (1974). Data for four specific stars,  $\beta$  Com,  $\epsilon$  Eri, 61 Cyg A, and 61 Cyg B, measured with 30 Å resolution were analyzed. It was judged that the problems associated with using lower resolution spectrophotometry were less significant for the red bandpass than for the violet bandpass. Thus, in this case we calibrated only the red pass band from the spectrophotometry, and used the mean  $C_{rv}$  relation to estimate the total continuum counts.

The results of these two calibrations are compared to Middelkoop's (1982) results in Figure 9. Considering the

problems associated with all three calibrations, the agreement is remarkably good for most of the  $B-V$  range of interest— $\lesssim 10\%$ . Middelkoop obtained a relation equivalent to

$$R_{\text{HK}} = 1.340 \times 10^{-4} C_{cf} S,$$

where  $\log C_{cf}(B-V) = 1.13(B-V)^3 - 3.91(B-V)^2 + 2.84 \times (B-V) - 0.47$ . (The factor  $1.34 \times 10^{-4}$  in the first equation above absorbs the Stefan-Boltzmann constant, as well as a normalizing factor of  $10^{14}$ , into Middelkoop's coefficient.) We have corrected  $C_{cf}$  for a non-physical maximum at  $B-V = 0.43$  by setting  $\log C'_{cf} = \log C_{cf} + \Delta \log C$ , where  $\Delta \log C = 0$  for  $B-V > 0.63$ , and  $\Delta \log C = 0.135x - 0.814x^2 + 6.03x^3$  for  $x \equiv 0.63 - (B-V) > 0$ . The quantity  $\log C'_{cf}$  is shown as the dashed, then solid line in Figure 9.

Eight of the program stars have been observed by Linsky et al. (1979). Their fluxes agree with ours to within  $\sim 20\%$ . The relatively large scatter may result from the difficulty of calibrating photographic slit spectra.

The worst discrepancy in the various attempts at calibration occurs for  $B-V \gtrsim 1.2$ . Vaughan and Preston (1980) noted that the color index for the continuum passbands,  $C_{rv}$ , shows an increasingly large scatter as a function of spectral type for  $B-V > 1.2$ . Thus we suspect that the disagreement in the calibrations reflects the increasing uncertainty in fluxes the heavily line-blanketed continuum bandpasses as a function of  $B-V$ . The O'Connell (1973) calibration may be the least

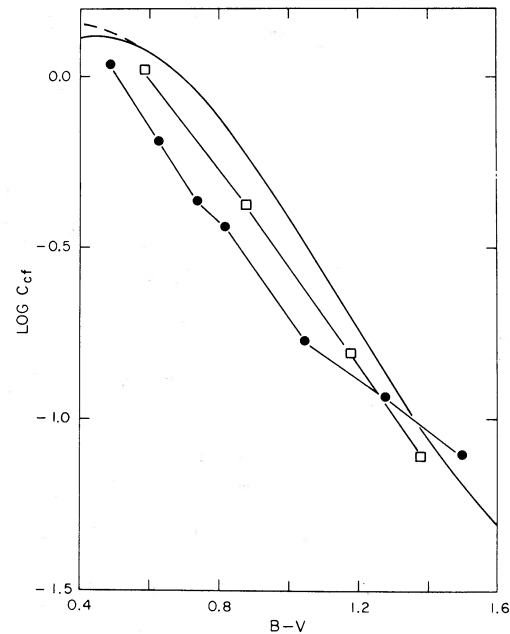


FIG. 9.—Relative comparison of different calibrations which convert the  $S$  index into the radiative loss ratio  $R_{\text{HK}}$  as a function of  $B-V$ , as described in the text. Solid line, Middelkoop's (1982) calibration; closed circles, a calibration based on O'Connell's (1973) spectrophotometry; open squares, a calibration based on the spectrophotometry of Faÿ et al. (1976); dashed line, extension of Middelkoop's (1982) calibration used in this paper. Vertical shifts of the calibrations are arbitrary.

accurate in this color range due to the combination of spectral types. We also note that  $B-V$  is not a good color index for very late dwarfs, and that the Barnes-Evans relation shows very large scatter for the coolest stars when expressed in terms of  $B-V$ .

Linsky *et al.* (1979) established an absolute calibration for continuum flux in the bandpass  $\lambda\lambda 3925-3975$ , as a function of  $V-R$  color, based on the Barnes-Evans relationship and the spectrophotometry of Willstrop (1964). Treating  $S$  as the residual intensity in the H and K lines, our calibration for  $R_{HK}$  implies a continuum flux in excellent agreement with that of Linsky *et al.* over the range  $0.45 \leq B-V \leq 0.90$ . For larger values of  $B-V$ , the Linsky *et al.* calibration falls below ours by an amount 0.3 dex at  $B-V = 1.25$ . Although the Linsky *et al.* continuum band is different from those in the Mount Wilson H-K spectrometer, disagreement by a factor of 2 seems large. For the present we employ the calibration given here and point out the need for further calibrations, perhaps using a different color index.

#### b) Correction of the HK Flux Ratio $R_{HK}$ for the Photospheric Contribution

The bandpass of the H-K spectrometer has a triangular shape as a function of wavelength, with a FWHM = 1.09 Å (Vaughan, Preston, and Wilson 1978). This bandpass is sufficiently wide to admit all of the chromospheric emission in the H and K lines of dwarf stars, but it also includes some flux from the stellar photosphere. Thus it is necessary to subtract the photospheric flux from the measured total flux in order to arrive at a true measure of chromospheric emission. This correction is unimportant for very late-type dwarfs, but is significant for the earliest spectral types considered here.

As is well known, the H and K lines can be interpreted in terms of an Eddington-Barbier analysis, in which the line profile maps out the temperature structure of the atmosphere. The flux exterior to the K1 and H1 minimum points, in the line wings, originates in the upper photosphere and is eliminated in our definition of chromospheric radiative losses. This convention defines "chromospheric" heating as that which occurs beyond the temperature minimum. Theoretical calculations indicate that most of the mechanical energy flux generated in the convective zone is damped in the upper photosphere (Stein 1967). There is observational evidence for this heating in the wings of the H and K lines (cf. White and Livingston 1981). Although we recognize that the chromospheric radiative losses may be only a small fraction of the total mechanical energy deposited, we restrict our attention to the strictly chromospheric component for practical reasons. The central emission reversal of the Ca II resonance lines varies much more than the wings (cf. White and Livingston 1981). As a result, the  $S$  index is much more sensitive to the chromospheric fraction of the radiative losses. Furthermore, the losses in Ca II are probably a much larger fraction of the total losses in the lower chromosphere than in the upper photosphere (Vernazza, Avrett, and Loeser 1981), so that even if we had accurate information about damping wing losses, the interpretation of such data would be very complicated.

Several authors have argued that, in addition to the obvious photospheric contribution exterior to the K1 and H1 minima, part of the flux in the line center is also photospheric in

origin. Blanco *et al.* (1974) suggested that the wing profiles can be extrapolated smoothly toward line center in order to define the photospheric level. Linsky and Ayres (1978, hereafter LA) showed that this procedure overestimates the photospheric component. Their results indicated that the Ca II line profiles for a model with no chromospheric temperature rise go to zero residual intensity at line center. LA suggested that only about 40% of the light between the K1 and H1 minima was photospheric in origin.

The local radiative loss for a specific line, in units of ergs  $\text{cm}^{-3} \text{s}^{-1}$ , is given by

$$\phi = hvA_{ul}N_u\rho_{ul},$$

where  $hv$  is the energy of the transition,  $A_{ul}$  is the transition probability,  $N_u$  is the population of the upper level, and  $\rho_{ul}$  is the net radiative bracket (Vernazza, Avrett, and Loeser 1981). The integral of  $\phi$  with height,

$$\Delta F = \int_h^\infty \phi dh$$

from the temperature minimum to infinity, is the total radiative loss in units of ergs  $\text{cm}^{-2} \text{s}^{-1}$ . From the radiative transfer equation in plane-parallel coordinates, the flux derivative is given by

$$dF/dz = \phi.$$

Hence  $\Delta F$  is the incremental flux originating in chromospheric layers, which appears in the emergent line profile. By an Eddington-Barbier argument, we expect most of  $\Delta F$  to appear within the line core.

Vernazza, Avrett, and Loeser (1981) have computed a simple chromospheric model intended to represent the average quiet Sun (their model C). The details of this calculation were kindly provided by Dr. E. Avrett. The flux profile in the Ca II K line and the radiative losses as a function of height in this line are shown in Tables 3 and 4. It is not exactly clear where to limit the integrations of the fluxes as a function of either height or wavelength. There is some ambiguity in determining the K1 minimum points in the line profile. Similarly, the net radiative losses turn negative just above the temperature minimum. Despite these uncertainties, Tables 3 and 4 clearly show that the total radiative losses in the Ca II K line above the temperature minimum correspond to approximately the total flux between the K1 points. We have also examined the results for the H line, and also for the H and K lines in different model chromospheres, finding essentially the same result.

The approximately equality of the total flux between the K1 minima and the total Ca II radiative losses in the model is due to the fact that the Ca II lines are thermalized near the temperature minimum (cf. Vernazza, Avrett, and Loeser 1981), so that most of the photons in the line core are produced above the temperature minimum. This suggests that essentially the entire flux within the K1 minima is produced above the temperature minimum.

The flux within the K1 minima approximately represents the total radiative losses in the K line in the chromosphere. This is true also in the LA analysis. However, LA take a further step by attempting to define the net, rather than the total, radiative losses from the chromosphere in the H and K

TABLE 3  
SOLAR FIVE LEVEL Ca II MODEL C  
K LINE FLUXES

$\Delta\lambda$	$F_\lambda$	$\int_{-\Delta\lambda}^{\Delta\lambda} F_\lambda d\lambda$
0.....	2.84 + 5	0
0.094...	4.69 + 5	6.37 + 4
0.151...	1.15 + 6	1.59 + 5
0.201...	8.67 + 5	2.62 + 5
0.251...	6.51 + 5	3.36 + 5
0.314...	5.67 + 5	4.12 + 5
0.377...	5.45 + 5	4.82 + 5
0.503...	5.64 + 5	6.22 + 5

TABLE 4  
MODEL C K LINE LOSSES

$h$	$T_e$	$\int_h^\infty \phi dh$
855.....	5650	3.85 + 5
755.....	5280	5.62 + 5
705.....	5030	6.19 + 5
655.....	4730	6.42 + 5
605.....	4420	6.28 + 5
555.....	4230	5.94 + 5
515.....	4170	5.60 + 5
450.....	4220	5.03 + 5

lines. They note that, in a radiative equilibrium model, some flux appears within the K1 and H1 minima in the absence of any nonradiative heating. These radiative losses are balanced by absorption of photospheric radiation. LA assume that the same absorption occurs in stellar chromospheres, and so they subtract the losses of the radiative equilibrium model from the total stellar chromospheric emission in order to compute the net energy loss which is to be balanced by mechanical heating.

It is not obvious, however, that the radiative heating within a stellar chromosphere can be estimated from the radiative heating of the corresponding radiative equilibrium atmosphere. It seems likely that many of the low-excitation atoms and molecules which might absorb photospheric radiation efficiently are destroyed at chromospheric temperatures. In addition, the contribution of a given ion may change from a net energy gain to a net loss, depending upon the local temperature. For example, Vernazza, Avrett, and Loeser (1981) show that the  $H^-$  ion in the solar chromosphere produces a net heating of the gas if the local temperature is  $< 4900$  K. That is,  $H^-$  absorbs more energy from the photosphere than it radiates. In principle, this absorption will heat the gas, helping to create Ca II emission in the absence of any nonradiative heating. However, Vernazza, Avrett, and Loeser (1981) show that if  $T > 5000$  K,  $H^-$  provides a net radiative loss. Under these conditions, for a given level of Ca II emission, nonradiative heating would have to be larger in order to balance the additional  $H^-$  losses.

We suggest that the radiative equilibrium procedure of

Linsky and Ayres (1978) may underestimate the nonradiative heating represented by the Ca II emission, because it assumes that some of the emission is balanced by photospheric heating processes not occurring at chromospheric temperatures. The response of the chromospheric emission to mechanical heating may be nonlinear; an increased mechanical energy flux may not produce a proportional increase in the Ca II emission.

Given the complexity of the problem, it seems safest to adopt a conservative definition of the photospheric radiation, namely, that it consists only of the radiation exterior to the H1 and K1 minima. This definition has the virtue of producing a clear way of determining the photospheric correction empirically.

We have estimated the amount of flux exterior to the H1 and K1 points measured by the HK photometer as a function of  $B-V$  for main-sequence stars. The derivation of the correction has been discussed by Hartmann *et al.* (1984). The results of this analysis can be expressed in the form

$$\log R_{\text{phot}} = -4.898 + 1.918(B-V)^2 - 2.893(B-V)^3$$

in the range  $0.44 < (B-V) < 0.82$ . We have also used the same expression for  $B-V > 0.82$ ; it becomes negligible for  $B-V \gtrsim 1.0$ . Hartmann *et al.* (1984) estimated a smaller photospheric contribution for  $B-V > 1.0$ ; however, the magnitude of the correction is less certain for the coolest stars, and in any case it is so small as to be relatively unimportant. When the photospheric corrections of the previously discussed Linsky and Ayres models are extrapolated to a bandpass of 1.09 Å and plotted versus  $B-V$ , they show a gradient with color nearly identical to the formula used here, and the present formula forms a lower bound to the Linsky and Ayres points. Use of the Linsky and Ayres values would not be expected to make a significant change in the conclusions drawn here; their photospheric correction is about 25% larger than ours on average.

In addition, we note that the analysis of Mg II emission for these stars (Hartmann *et al.* 1984) indicates a good correlation between Mg II and Ca II losses. Furthermore, the ratio of Ca II to Mg II emission is independent of spectral type, which would not be true if we adopted a significantly larger photospheric correction.

In an independent analysis, one of us (D. D.) recently obtained an alternative form for the photospheric correction, which fits the one used in this paper to within observational errors:

$$\log R_{\text{phot}} = -4.02 - 1.40(B-V).$$

Because of its simple form, this expression may be preferable for future use.

We note that subtraction of  $R_{\text{phot}}$  from the total H-K emission  $R_{\text{HK}}$  does not have a large effect for active chromosphere stars, but it can be a very significant correction for the chromospherically less active stars. For these stars in particular it is important to determine the photospheric correction more rigorously than has been done here, both by extending the sample of stars with calibrated H-K profiles and by carrying out model chromosphere calculations, similar to those described above for the Sun, for other spectral types on the lower main sequence.

## REFERENCES

- Allen, C. W. 1973, *Astrophysical Quantities* (London: Athlone).
- Baker, W. H., and Temesvary, S. 1966, *Tables of Convective Stellar Envelope Models* (2d ed.; New York: NASA/Goddard Institute for Space Studies).
- Baliunas, S. L., Hartmann, L., Vaughan, A. H., Liller, W., and Dupree, A. K. 1981, *Ap. J.*, **246**, 473.
- Baliunas, S. L., Vaughan, A. H., Hartmann, L., Middelkoop, F., Mihalas, D., Noyes, R. W., Preston, G. W., Frazier, J., and Lanning, H. 1983, *Ap. J.*, **275**, 752.
- Barnes, T. G., and Evans, D. S. 1976, *M.N.R.A.S.*, **174**, 489.
- Blanco, C., Catalano, S., Marilli, E., and Rodono, M. 1974, *Astr. Ap.*, **33**, 257.
- Berthomieu, G., Cooper, A. J., Gough, D. O., Osaki, Y., Provost, J., and Rocca, A. 1980, in *Non-Radial and Nonlinear Stellar Pulsation*, ed. H. A. Hill and W. A. Dziembowski (New York: Springer), p. 307.
- Catalano, S., and Marilli, E. 1983, *Astr. Ap.* **121**, 190.
- Chugainov, P. F. 1980, *Isv. Krymsk. Ap. Obs.*, **61**, 124.
- Duncan, D. 1981, *Ap. J.*, **248**, 651.
- Duncan, D., Baliunas, S. L., Noyes, R. W., and Vaughan, A. H. 1984, *Pub. A.S.P.*, to be submitted.
- Durney, B. R., and Latour, J. 1978, *Geophys. Ap. Fluid Dyn.*, **9**, 241.
- Durney, B. R., Mihalas, D., and Robinson, R. 1981, *Pub. A.S.P.*, **93**, 537.
- Durney, B. R., and Robinson, R. D. 1982, *Ap. J.*, **253**, 290.
- Fay, T. D., Jr., Stein, W. L., and Warren, W. H., Jr. 1974, *Pub. A.S.P.*, **86**, 772.
- Gehren, T. 1982, *Astr. Ap.*, **109**, 187.
- Gilman, P. 1980, in *IAU Colloquium 51, Stellar Turbulence*, ed. D. Gray and J. Linsky (New York: Springer), p. 19.
- Hartmann, L., Soderblom, D., Noyes, R., Burnham, N., and Vaughan, A. 1984, *Ap. J.*, **276**, 254.
- Johnson, H. L. 1966, *Ann. Rev. Astr. Ap.*, **4**, 193.
- Knobloch, E., Rosner, R., and Weiss, N. O. 1981, *M.N.R.A.S.*, **197**, 45P.
- Kraft, R. P. 1967, *Ap. J.*, **150**, 551.
- Krause, F., and Radler, K. H. 1980, *Mean Field Electrodynamics and Dynamo Theory* (Oxford: Pergamon).
- Leighton, R. B. 1959, *Ap. J.*, **130**, 366.
- Linsky, J. L., and Ayres, T. R. 1978, *Ap. J.*, **220**, 619 (LA).
- Linsky, J. L., Worden, S. P., McClintock, W., and Robertson, R. M. 1979, *Ap. J. Suppl.*, **41**, 47.
- Lubow, S. H., Rhodes, E. J., Jr., and Ulrich, R. K. 1980, in *Non-Radial and Nonlinear Stellar Pulsation*, ed. H. A. Hill and W. A. Dziembowski (New York: Springer), p. 300.
- Middelkoop, F. 1982, *Astr. Ap.*, **107**, 31.
- Moffat, H. K. 1978, *Magnetic Field Generation in Electrically Conducting Bodies* (Cambridge: Cambridge University Press).
- Noyes, R. W. 1983, in *IAU Symposium 102, Solar and Stellar Magnetic Fields: Origins and Coronal Effects*, ed. J. O. Stenflo (Dordrecht: Reidel), p. 133.
- O'Connell, R. W. 1973, *A.J.*, **78**, 1074.
- Pallavicini, R., Golub, L., Rosner, R., Vaiana, G., Ayres, T., and Linsky, J. 1981, *Ap. J.*, **248**, 279.
- Parker, E. N. 1979, *Cosmical Magnetic Fields: Their Origin and Their Activity* (Oxford: Clarendon Press).
- Radick, R. R., Hartmann, L., Mihalas, D., Worden, S. P., Africano, J. I., Klimke, A., and Tyson, E. T. 1982, *Pub. A.S.P.*, **94**, 934.
- Robinson, R. D., and Durney, B. R. 1982, *Astr. Ap.*, **108**, 322.
- Skumanich, A., and Eddy, J. 1981, in *Solar Phenomena in Stars and Stellar Systems*, ed. R. M. Bonnet and A. K. Dupree (Dordrecht: Reidel), p. 349.
- Skumanich, A., Smythe, C., and Frazier, E. N. 1975, *Ap. J.*, **200**, 747.
- Soderblom, D. 1983, *Ap. J. Suppl.*, **53**, 1.
- Stein, R. F. 1967, *Ap. J.*, **154**, 297.
- Stimets, R. W., and Giles, R. 1980, *Ap. J. (Letters)*, **242**, L37.
- Vaiana, G., et al. 1981, *Ap. J.*, **245**, 163.
- Vaughan, A. H. 1980, *Pub. A.S.P.*, **92**, 392.
- . 1983, in *IAU Symposium 102, Solar and Stellar Magnetic Fields: Origins and Coronal Effects*, ed. J. O. Stenflo (Dordrecht: Reidel), p. 113.
- Vaughan, A. H., Baliunas, S. L., Middelkoop, F., Hartmann, L. W., Mihalas, D., Noyes, R. W., and Preston, G. W. 1981, *Ap. J.*, **250**, 276.
- Vaughan, A. H., and Preston, G. W. 1980, *Pub. A.S.P.*, **92**, 385.
- Vaughan, A. H., Preston, G. W., and Wilson, O. C. 1978, *Pub. A.S.P.*, **90**, 267.
- Vernazza, J. E., Avrett, E. H., and Loeser, R. 1981, *Ap. J. Suppl.*, **45**, 635.
- Walter, F. M. 1981, *Ap. J.*, **245**, 677.
- . 1982, *Ap. J.*, **253**, 745.
- White, O. R., and Livingston, W. C. 1981, *Ap. J.*, **249**, 798.
- Willstrop, R. V. 1964, *Mem. R.A.S.*, **69**, 83.
- Wilson, O. C. 1978, *Ap. J.*, **226**, 379.

S. L. BALIUNAS, L. W. HARTMANN, and R. W. NOYES: Center for Astrophysics, 60 Garden Street, Cambridge, MA 02138

D. K. DUNCAN: Mount Wilson and Las Campanas Observatories, 813 Santa Barbara Street, Pasadena, CA 91101-1292

A. H. VAUGHAN: Applied Optical Division, Perkin-Elmer Corp., P.O. Box 3115, Garden Grove, CA 92642